agriculture

MDPI

Article

Design and Experimental Study of a Biomimetic Pod-Pepper-Picking Drum Based on Multi-Finger Collaboration

Chuanxing Du, Weiquan Fang, Dianlei Han, Xuegeng Chen and Xinzhong Wang *

School of Agricultural Engineering, Jiangsu University, Zhenjiang 212013, China; 2212016041@stmail.ujs.edu.cn (C.D.); 2112116003@stmail.ujs.edu.cn (W.F.); handianlei@ujs.edu.cn (D.H.); 1000005204@ujs.edu.cn (X.C.)

* Correspondence: xzwang@ujs.edu.cn; Tel.: +86-13852989966

Abstract: In order to reduce ground drop loss during mechanical pepper picking and improve the net recovery rate, a drum snap finger picking device was designed. The picking device is mainly composed of a picking drum and auxiliary picking components; the picking finger arrangement was designed biomimetically and its structure and operating parameters were optimized by the DEM (discrete element method). According to the physical and mechanical characteristics of the pepper and the simplified three-dimensional model of the picking device, a virtual simulation model of the pepper-picking device was established using the EDEM software. Through simulation analysis and using the orthogonal test method, the main factors which affect the ground drop loss rate of pepper and their optimal parameter combination values were determined. The simulation results were verified by a pepper-picking field experiment. Orthogonal tests show that, when the picking drum speed (V') is 210 rpm, the pepper-feeding speed (V'') is 1100 mm·s^{-1}, the bending angle of each picking spring tooth (C) is 162°, and each group of circumferential fingers has rows, the picking device has a good picking effect. At this time, the ground drop loss rates in both the simulation and field test were 7.50% and 7.85%, respectively, and the drop error was only 4.46%, which was within the allowable range. The design form and parameter optimization simulation method in this paper provide an important reference for the design and optimization of pepper-harvesting machinery.

Keywords: bionic design; pod pepper; picking device; ground drop loss; orthogonal test method

Citation: Du, C.; Fang, W.; Han, D.; Chen, X.; Wang, X. Design and Experimental Study of a Biomimetic Pod-Pepper-Picking Drum Based on Multi-Finger Collaboration. *Agriculture* **2024**, *14*, 314. https://doi.org/10.3390/agriculture14020314

Academic Editor: José Lima

Received: 2 January 2024
Revised: 26 January 2024
Accepted: 14 February 2024
Published: 16 February 2024

1. Introduction

Pepper is planted widely in China in provinces such as Jiangsu, Henan, Sichuan, and Guizhou. To improve the picking rate of pod peppers, the development of a pepper-picking device suitable for the mechanized harvesting of peppers is needed. The main picking devices for pepper harvesting are as follows: the double-helix picker, which uses a double helix rod to continuously rub, beat, and comb the peppers; the long-rod comb picker, by which peppers are picked by tapping peppers with shafts equipped with rod-like teeth [1]; the ribbon comb picker, where a picking belt and the upper comb teeth move from bottom to top to remove peppers from their stems [2]; and the drum snap finger picker, in which a picking drum with staggered picking fingers on it rotates at a high speed, and the peppers are fed into it and pass through the gaps between the adjacent fingers on the front and back, and are plucked from the stems using a friction comb on the side wall of the fingers. The unfolded double-helix picking device and the long-stem comb-tooth picking device are also suitable for picking pepper varieties with large fruits, such as American green peppers and dried red peppers, but they are not effective when picking peppers with small diameters, such as thread peppers and pod peppers. The double-helix picking device and the band-shaped comb-tooth picking device have the characteristic of parallel operation, which makes them unsuitable for complex pepper cultivation in small fields.

Currently, pepper-picking machines are gradually developing towards automation. Ning et al. conducted path planning for an automatic chili-picking device [3]. Liu used

deep cameras and deep learning algorithms for recognition and localization during the pepper-picking process [4]. Picking methods based on intelligent algorithms have high picking accuracies. Deng et al. designed a flexible and effective method for chili picking [5]. The drum snap finger picking device has the advantages of picking flexibility and high variety adaptability. It can achieve non-aligned picking and can adjust the picking fingers' spacing to adapt to pepper varieties with different diameters. The drum snap finger picking device has the advantages of simple structure, continuous operation, high flexibility, high operating efficiency, and wrong operation, and has gradually become one of the key technologies of mechanized harvesting equipment for pepper in China. However, domestic research mainly focuses on the structural design and performance testing of the whole machine. The structure and material design of picking fingers are similar, and simple steel structures are used more often, resulting in a high pepper breakage rate. At the same time, the collaborative arrangement scheme of picking fingers is not well-studied, resulting in a large loss of peppers to ground drop in the existing self-propelled pepper-picking device. In order to improve the harvesting rate of the drum snap finger picking device and reduce the loss rate of crops, some scholars have taken the combination of agricultural machinery and agronomy as a foothold and conducted research on loss reduction by improving key components and optimizing operating parameters. Xie et al. used rod teeth made from flexible materials instead of rigid rod teeth, which reduced the loss rate of rice grain threshing [6]. Zou et al. designed a nylon finger to replace the traditional steel wire finger for pepper and plate pepper [7]. Field tests show that the nylon finger is significantly better than the steel wire finger at reducing the breakage rate. Bionic threshing components draw on animal behavior or mechanisms that have efficient threshing ability and do not easily cause crop loss in nature, which helps to improve the grain removal rate and reduce threshing loss [8–13]. For example, Li et al. took inspiration from the action of chickens pecking corn, took the rooster's beak structure as the bionic prototype, refined its geometric structure and morphological features, and designed a corn bionic threshing roller, which improved the decontamination rate of corn kernels and reduced the loss of corn [8]. Islam et al. used a robotic arm for chili picking and optimized the parameters through kinematic analysis [14], and through machine vision, the accuracy of the robotic arm picking was effectively improved [15]. By analyzing and planning the movement trajectory of picking devices and other devices, the accuracy of picking devices can also be improved [16,17].

In order to improve the collection rate and reduce the breakage rate of the pepper-picking drum, the bionic finger snapping device and multi-finger synergistic bionic finger arrangement scheme on the picking drum were designed in this paper, and then a roller finger snapping pepper-picking device was designed. Based on the physical and mechanical parameters and discrete element model of pod peppers, a simulation model of a pepper-picking bench was established, and the picking parameter combination with the smallest ground drop loss rate of peppers was optimized through the quadratic rotational orthogonal test of the response surface. The field test results further verified the feasibility of the collaborative multi-finger drum-snapping picking arrangement scheme, which was helpful for reducing ground drop loss when mechanically picking peppers.

2. Materials and Methods

2.1. Overall Structure of the Picking Device

The picking device is the picking part of the pepper harvester, which is responsible for feeding, picking, and transporting the pepper, which directly affects the harvesting efficiency and quality of the machine. The picking device (Figure 1) is mainly composed of a ground-profiling wheel, picking roller, pepper-pressing wheel, pepper divider, roller-upper baffle, picking frame, inclined conveyor belt, material blocking plate, elevator conveyor belt, lifting cylinder, transmission system, etc. When the harvester advances, the pepper plants are fed into the picking device by the pepper divider, and the peppers are pushed down and sent into the picking drum by the pepper-pressing wheel. The picking drum consists of many regularly arranged picking snap finger and drum shaft frames. When

working, the transmission system drives the picking drum to rotate clockwise at high speed, and the pepper is picked from the pepper plant under the friction, brushing, and knocking of the picking finger and its side wall, and is thrown along the rotating direction of the drum in a parabolic path onto the conveyor belt.

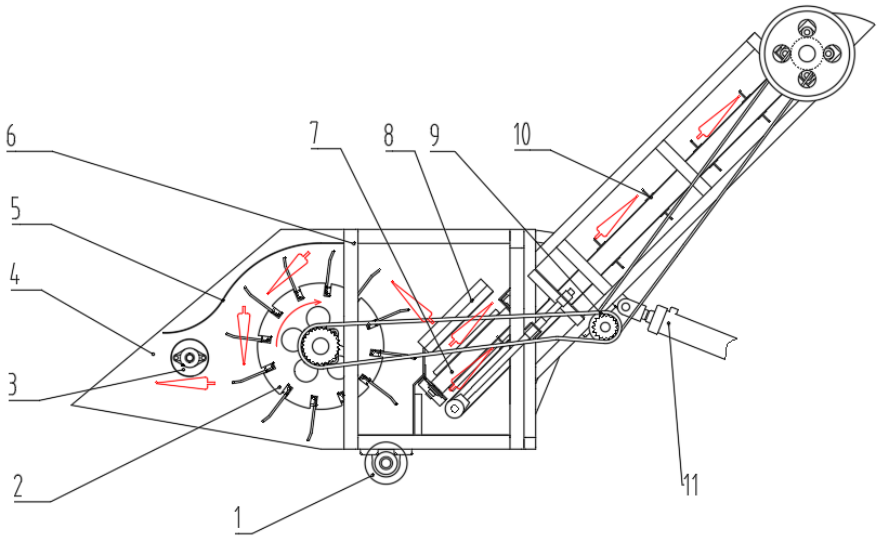

Figure 1. Overall structure diagram of the pepper-picking device. 1. Ground-profiling wheel. 2. Picking drum. 3. Pepper-pressing wheel. 4. Pepper splitter. 5. Roller-upper baffle. 6. Picking rack. 7. Diagonal conveyor belt. 8. Baffle. 9. Transmission system. 10. Elevator conveyor belt. 11. Lifting cylinder.

The picking drum is the core picking part of the picking device, and the drum structure should be adapted to the agronomic characteristics of pod pepper. The pepper used in the experiment is Sanying pod pepper grown in Shouxian Town, Feng County, Jiangsu Province, China. As shown in Figure 2, the average row spacing is 720 mm, and the average plant width is 228 mm. At the same time, two rows of peppers were harvested, and the width (B) of the picking drum was 1700 mm. As shown in Figure 2, in order to ensure that all pod peppers are picked on the plant, the diameter of the picking drum (D) and the installation height of the drum shaft (H) should meet the quantity relationship in Equation (1), D $\geq$ 249 mm should be solved, and D should be 800 mm; 203 $\leq H \leq$ 774, and H was taken as 600 mm.

$$\begin{cases} H - \frac{D}{2} \leq L \\ H + \frac{D}{2} \geq U \end{cases} \quad (1)$$

where H is the installation height of the axis of the picking drum, mm; D is the diameter of the picking drum, mm; L is the minimum height of the pepper fruit from the ground, which is 364 mm; U is the highest height of the pepper fruit from the ground, which is 613 mm. (The data were obtained from field measurements in the farmland).

In order to improve the picking efficiency, all peppers should be fed into the picking drum by the pepper-pressing wheel intensively, and its installation position should meet the quantity relationship in Equation (2). The solution should obtain h > 454 mm, and h was taken as 460 mm. M > 400 mm, and M was taken as 450 mm. The diameter of the pepper-pressing wheel should not be less than the maximum length (S) of pepper-to-buffer feeding to reduce the splash loss of pepper, so its diameter is 150 mm. The pepper splitters on both sides and the pepper-pressing wheel concentrate the peppers on the plants in a rectangular area of 1700 $\times$ 100 mm^2 and feed them into the picking drum to improve the picking efficiency.

$$\begin{cases} h - L > S \\ M > \frac{D}{2} \end{cases} \quad (2)$$

where h is the height of the lowest point of the pepper-pressing wheel from the ground, mm; L is the lowest height of the pepper fruit from the ground, measuring 364 mm; S is the maximum length of pod pepper (with short stems), 90 mm; M is the horizontal distance of the rightmost point of the pepper-pressing wheel from the axis of the picking drum, mm; D is the diameter of the picking drum, 800 mm.

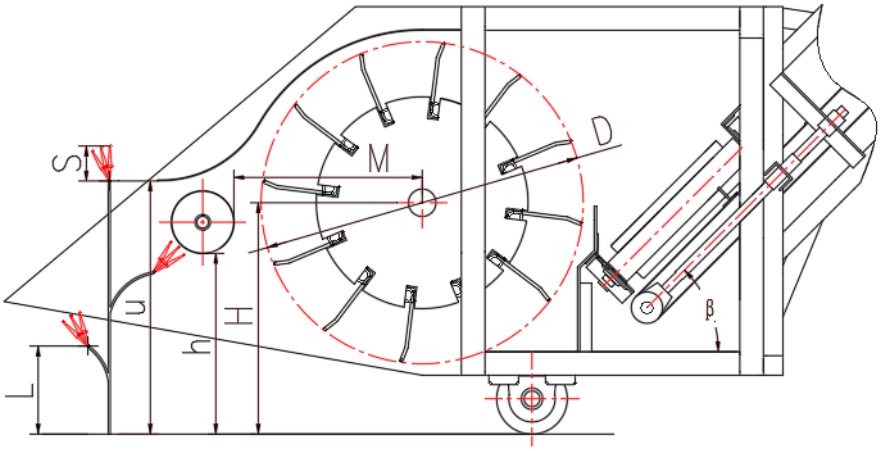

Figure 2. Schematic diagram of the main structure and parameters of the picking device.

2.2. Analysis of Human Finger Configuration and Posture of Picking Peppers

The shape of the human hand is simple, mainly composed of the wrist, palm, and fingers, and it is one of the most intelligent and unique organs on the human body. Most of a human's powerful hands-on practical ability comes from the fine control of wrist and fingers and their movement configuration. When human fingers pick peppers (Figure 3), the stalks and pepper siliques pass through the gaps of the five fingers with 21 degrees of freedom; the thumb and the other four fingers grip the peppers and move toward the palm in an enclosed configuration. The peppers are picked from the plants under certain knuckle flexion and wrist backward movement speed, as well as the friction, brushing, and tapping of multiple fingers. Multi-finger cooperative arrangement and joint movement configuration gesture of the fingers makes it easy for humans to deal with the task of picking peppers of various shapes, which not only ensures the smooth picking of peppers, but also avoids the loss of peppers falling on the ground.

Figure 3. Pepper-picking posture of multi-finger synergistic joint movement of human hands.

2.3. Multi-Finger Collaborative Arrangement Scheme for Picking Fingers

The picking drum of the pod-pepper-picking device is mainly composed of a drum shaft frame and multiple rows of snap fingers evenly distributed around the drum. A schematic diagram of the multi-finger collaborative arrangement scheme of picking fingers is shown in Figure 4. The picking drum consists mainly of a drum shaft frame and multiple rows of snap fingers evenly distributed around the drum. In order to ensure the force balance of the drum during high-speed rotation, the total number of finger rows on the drum was selected as an even row, and considering the characteristics of the cycle of the dislocation of the finger of the circumferential row, it was determined that the total number of the last week of the drum (G) should be 12 rows (12 is a multiple of 2, 3, and 4). The picking finger arrays of each row in the axial direction were arranged to ensure that the distance between the adjacent finger trunks is equal. Each circumferential row upwards refers to the unit of the group (total group is $\frac{12}{N}$), and each group row spiral circular arrangement (N). And the axial center distance of the adjacent finger trunk of the adjacent finger in the circumferential row is ensured to be equal everywhere. The specific position relationship should satisfy the quantity relationship in Equations (3)–(7) to ensure the smooth picking of pod pepper.

$$P = N \cdot l \tag{3}$$

$$t = l - D' = \frac{P}{N} - D' \leq d \tag{4}$$

$$A = \frac{2\pi}{G} \tag{5}$$

$$K = \frac{\pi D}{G} \tag{6}$$

$$NK = N \times K \tag{7}$$

where P is the axial center distance of adjacent finger stems, mm; N is the number of finger rows in each group in the circumferential direction, which can be 2, 3, or 4; t is the axial distance between adjacent fingers in the circumferential direction, mm; l is the axial center distance between adjacent knuckles in the adjacent rows of fingers, mm; D' is the outer diameter of the finger stem of the picking fingers, 8 mm; d is the minimum diameter of the silique of pod pepper, measured at 7 mm; A is the installation angle of the adjacent rows of fingers in the circumferential direction, rad; G is the total number of rows of fingers on the drum, initially determined to be 12; K is the maximum arc length distance between adjacent rows of fingers in the circumferential direction, mm; D is the diameter of the picking drum, which has been determined to be 800 mm; NK is the arc distance of two adjacent groups of fingers, mm.

The arrangement scheme of picking fingers when the number N (N = 2, 3, 4) of each group of fingers in the circumferential direction takes different values is shown in Figure 5. Under the premise that the width of the drum (B) and the diameter of the picking drum (D) remain unchanged, and the quantitative relationship in Equation (3) is satisfied, changing the number of rows of each group of snap fingers (N) in the circumferential direction can simultaneously change the axial center distance (P) between the adjacent fingers of each row of snap fingers and two adjacent groups of flicking arc distance (NK). When the influencing factors such as the rotating speed of the picking drum, the feeding speed of pod peppers, and the bending angle of the fingers are constant, the size of NK directly affects the frequency of combing, tapping, and friction of the picking fingers on the peppers, which may affect the picking ground drop loss rate of pod peppers.

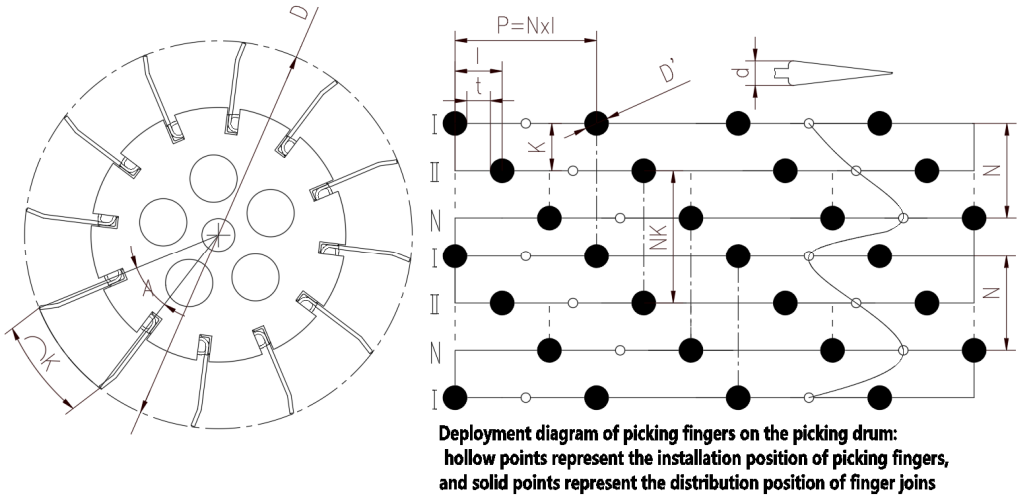

Figure 4. Schematic diagram of multi-finger collaborative arrangement scheme for picking fingers.

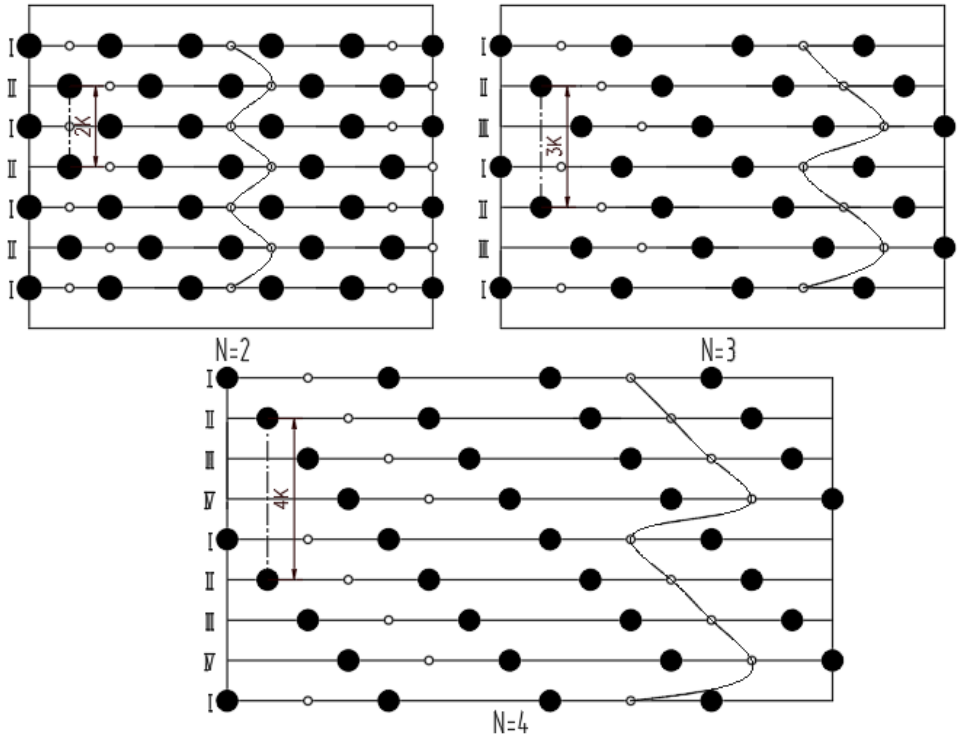

Figure 5. Schematic diagram of picking finger arrangement at different times for each group of circumferential finger rows.

Based on the above joint movement scheme of picking finger co-arrangement, four parameter factors that may have a significant impact on the ground drop loss rate of pod pepper are proposed for study, namely picking drum speed (V'), pod pepper feeding speed (V''), number of finger rows (N) in each group of the circumferential direction, and finger bending angle (C) of the picking finger, as shown in Figure 6. As shown in Figure 6, the finger joint in the figure imitates the bending of the human finger joint (Figure 6c). In the layout design of the picking drum, it imitates the collaborative operation of multiple fingers in the human body, thus imitating the process of picking pod peppercorns with human fingers.

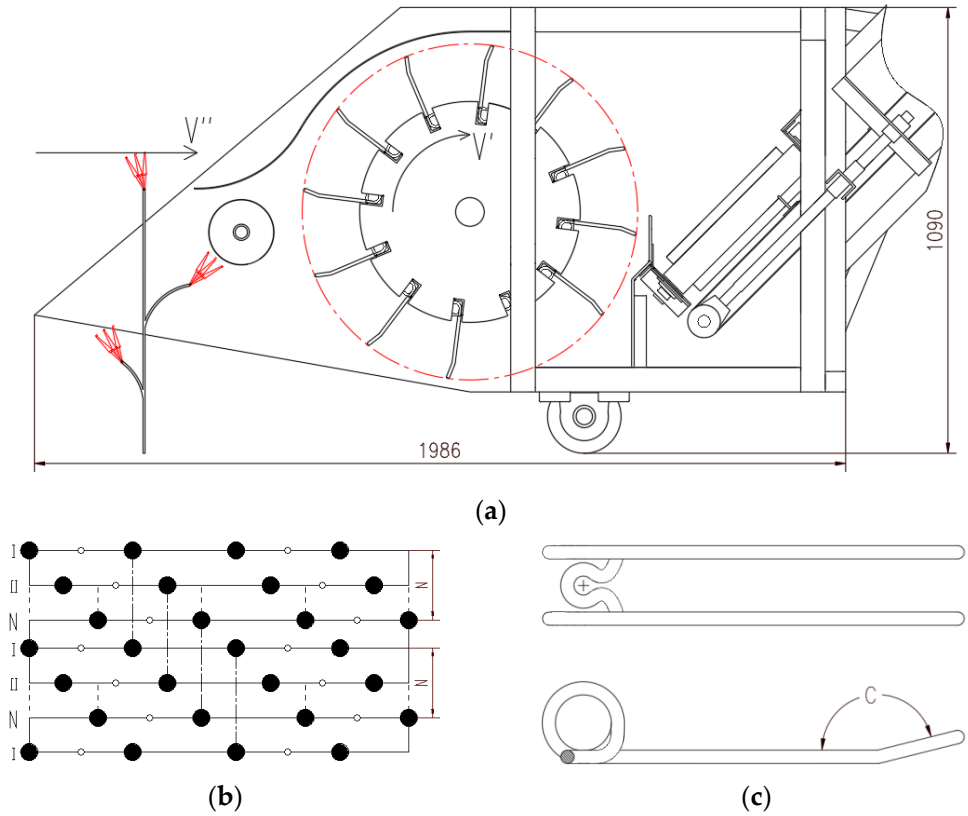

Figure 6. Schematic diagram of influencing factors of ground drop loss rate of pod pepper. (**a**) Schematic diagram of the working parameters of the picking device; (**b**) arrangement scheme of bionic snap fingers; (**c**) structural diagram of picking snap fingers. V' is picking drum rotation speed; V'' is pod pepper feeding speed; N is number of rows of fingers in each group; C is bending angle of picking fingers.

When the picking device is working, the picking drum rotates clockwise at a speed of 150 to 250 rpm to pick peppers. The harvesting machine harvests at a working speed of 1.8–5.4 km·h^{-1}. To ensure that the pepper is fed into the picking device, the horizontal feeding speed was set as 500–1500 mm·s^{-1}. The row number (N) of each group of snap fingers in the circumferential direction (N is taken as 2, 3, or 4) is a key parameter affecting the collision frequency between picking snap fingers and peppers. Picking finger bending angle (C) affects the picking trajectory and posture of pepper. It is preliminarily determined that its value range should be 90–180°.

2.4. EDEM Simulation Model of Pepper-Picking Platform

2.4.1. Determination of Discrete Element Simulation Parameters

Therefore, in the simulation process, the deformation of pepper was considered to be ignored, and the discrete element model of pepper particles was regarded as not deformed. Therefore, the selection of the Hertz–Mindlin (no slip) contact model and the Standard Rolling Friction model can better simulate the actual contact collision situation and speed up the simulation process [18]. The discrete element model of pod pepper was established by filling the particle template with a multi-sphere model (Figure 7c). The corresponding particle properties were assigned according to the physical and mechanical research data of pod pepper (Table 1) [19]. The discrete element parameters of pod pepper required for biomimetic tooth simulation are shown in Table 1. The accuracy of simulation parameters and the established pepper model was verified by the pumping method (Figure 7).

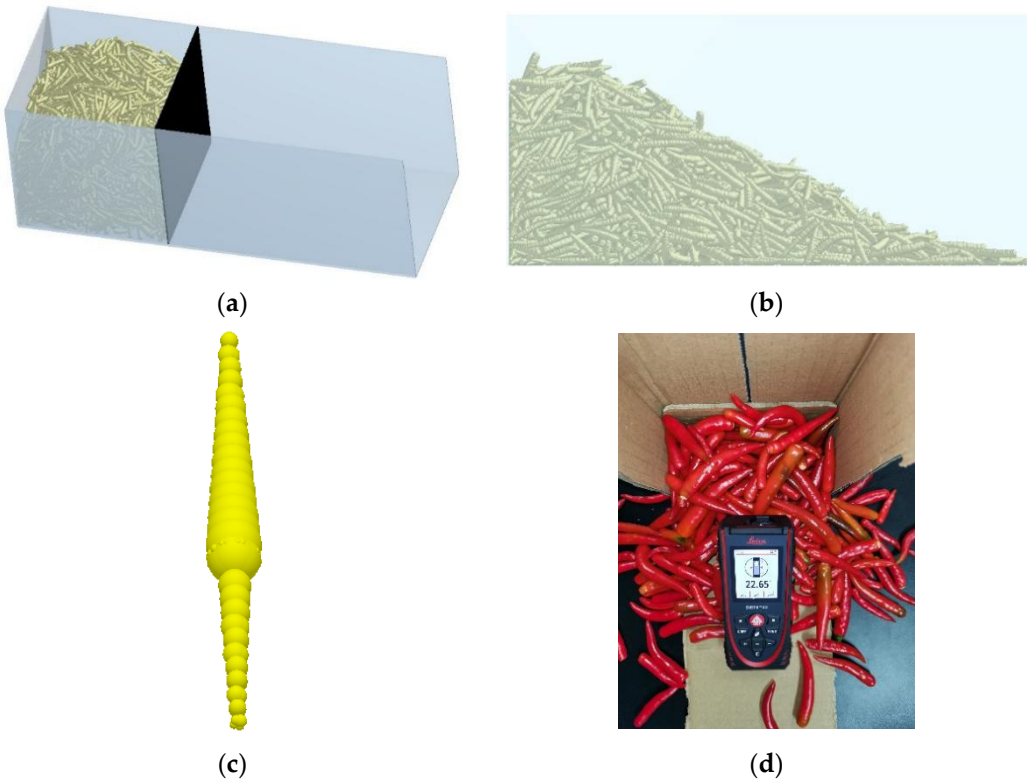

Figure 7. Pepper discrete element parameters and model validation. (**a**) Before drawing the board; (**b**) after pumping; (**c**) pepper discrete element model; (**d**) pulling plate test.

Table 1. Values of parameters required for the simulation test.

Simulation Parameter Category	Parameter	Value
Intrinsic parameters of pod pepper	pod pepper Poisson's ratio	0.40
	pod pepper particle density (kg·m^{-3})	7.6×10^2
	pepper shear modulus (MPa)	0.85
Contact parameters of pod pepper	pod–pod collision recovery coefficient	0.36
	pod–steel plate collision recovery coefficient	0.42
	pod–steel plate static friction coefficient	0.39
	pod–steel plate rolling friction coefficient	0.19
Material parameters of steel	steel density (kg·m^{-3})	7.85×10^3
	Poisson's ratio of steel	0.30
	shear modulus of steel (MPa)	8×10^4

2.4.2. Establishment of Discrete Element Simulation Model

To reduce the simulation time, the width of the picking drum was reduced to 500 mm, and SolidWorks 2020 was used to build the three-dimensional model of the pepper-picking platform, as shown in Figure 8. This model removes extraneous structures, but retains necessary components such as the pepper-pressing wheel, the upper baffle on the drum, and the picking drum. And on the original picking frame, the front baffle of the drop area, partition baffle, collection area baffle, and other closed baffles were added, and the internal space of the bench model was divided into "collection area" and "drop area".

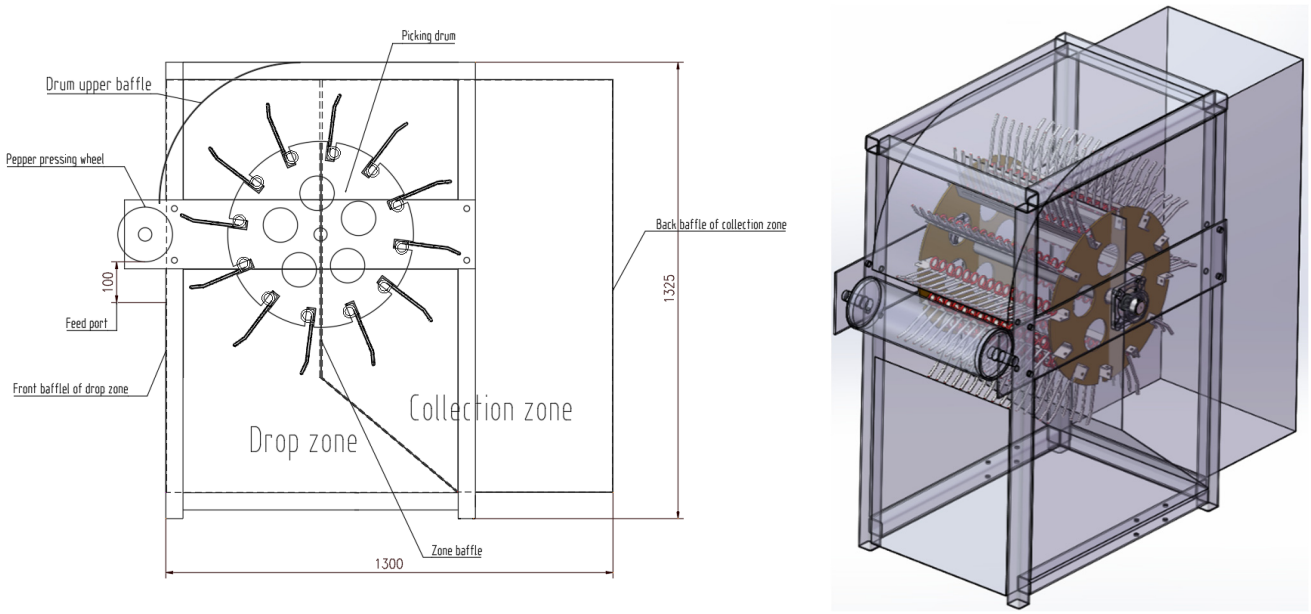

(**a**) (**b**)

Figure 8. Two-dimensional and three-dimensional model of pod-pepper-picking platform. (**a**) Two-dimensional model; (**b**) three-dimensional model.

During the simulation, a large number of pepper pellets were randomly generated at the feed inlet (mm^2, rectangular area) on the left side of the bench model through the pellet factory, and a rightward horizontal feeding speed (V'') was applied to these pellets. Under the picking action of the high-speed rotation of the picking drum, most of the pepper particles were thrown behind the bench model and fell to the "collection area" due to gravity, which was regarded as successful harvesting. A small number of unsuccessfully harvested peppers were blocked by the partition baffle and the front baffle of the drop area in the left half of the bench model, and finally fell to the "drop area", which was regarded as a ground drop loss.

EDEM 2021.2 is a general-purpose CAE software based on the discrete element method for simulating the behavioral characteristics of granular systems of bulk materials. It defines and quickly performs dynamic analysis of bulk material systems. In the EDEM simulation, many discrete pepper particles were randomly generated at the feed port (rectangular plane) on the left side of the bench model through the particle factory, and a horizontal feeding speed to the right was applied to these pepper particles. Most of these pepper particles were thrown behind the bench under the high-speed rotation of the picking drum and fell to the "harvesting area" due to gravity, which was considered successful harvesting. A small number of unsuccessfully harvested peppers were blocked by the partition baffle and the front baffle of the drop area in the left half of the bench model, and finally fell to the "drop area", which was regarded as a ground drop loss. Through multiple picking bench EDEM simulation pre-tests, it was found that EDEM can better meet the test requirements when dealing with the relative motion of the picking drum, partition baffle, and pepper particles.

EDEM 2021.2 was used to carry out the simulation experiment of the pepper-picking bench; the specific steps are mainly divided into three parts: pre-processor, solver, and post-processor. The pre-processing module can complete the establishment of the pod pepper discrete element model, the assignment of physical mechanics and contact attributes, pre-simulation preparations such as the import of the picking bench geometry, the generation of the particle factory, and the selection of the contact model. In the solver part, the setting of the Rayleigh time step for the solution, simulation time, data saving time interval, selection of the solver engine, start the simulation, etc., can be completed. After the simulation is over, the quantity or quality of peppercorns in the "drop zone" and "collection zone" can

be visually monitored through the post-processing module, so as to obtain the drop loss rate of peppercorns in each simulation test.

(1) Pre-treatment. Since the connection force between the short stem and the plant of pod pepper is much smaller than that of pod pepper at the fruiting force [20], when picking rollers to harvest pepper, the fruit of the pepper is often picked together with the short stem (with the handle). Therefore, in the simulation process, it is proposed to establish an integrated discrete element model of pod pepper stem, and the physical and mechanical properties of the short stem were regarded as the same as those of pod pepper fruit. According to the 3D measurement data of pod pepper and short stem stalk, an integrated 3D model of pepper with handle was established, and it was imported into EDEM 2021.2 software as a particle filling template.

The 3D model of the pod-pepper-picking platform established above was imported into EDEM 2021.2 as geometries as well as the material properties of steel, and the contact properties between geometry and the pod pepper can be set. The merge function in geometry was used to fuse the picking drum parts into one drum geometry and merge the rest of the racks into another rack geometry, and add a clockwise linear rotation speed (V') around the drum axis to the drum. At the fixed position (−715, 324, 2315) at the feed inlet in front of the bench model, a virtual box geometry was established as a particle factory, and a total of 216 pod pepper particles with handles were randomly generated in a dynamic manner. Through the mass calculation function of EDEM, the total mass of the particles (m_{z1}) is 373.7 g, which is less than the actual weight of 100 grains of pod pepper, which is 708.3 g. This is because the volume of the pod pepper model is larger than the actual volume in the process of 3D modeling and discrete element model particle filling was reduced. The feeding velocity is flat in the −X direction, and the number of hot peppers generated per second and the simulation time were dynamically adjusted in proportion to the size, so as to achieve the same feeding amount and feeding effect as the actual picking operation. In the actual picking process, the stress deformation and the huge picking movement speed and movement distance of pod pepper are relatively small, and have little impact on the picking results, and the main consideration index of the simulation process is the ground drop loss of pepper. The acceleration of gravity was set to $-9.81\ \mathrm{m{\cdot}s^{-2}}$ in the Y direction.

(2) Solver. The simulation fixed time step was set to 20% in the solver module, and the simulation time was dynamically adjusted to 2~4 s according to the feeding speed of pepper, so as to ensure that all pepper particles are generated and "harvested". The cell size was set as 2.5 R, and the GPU solution engine was selected to speed up the solution. The schematic diagram of the simulation process of the pepper-picking platform is shown in Figure 9.

(3) Post-processing. After the simulation is completed, we switch to the post-processing module, and in the Setup Selections analysis function, import a Geometry Bin Group 3D model of the same size as the "collecting area" to monitor the quality of the harvested pod peppers, and adjust the model position coordinates so that it coincides with the "collection area". As shown in Figure 10, the monitoring item was set to the total mass of pod pepper in the Geometry Bin Group area, and this part of the mass (for example, shown in the figure is 275.967 g) is the mass of pod pepper successfully harvested during the simulation process, then the ground drop loss mass and ground drop loss rate of pod pepper in the simulation can be determined by Equation (8).

$$\begin{cases} m_{g1} = m_{z1} - m_{s1} \\ \eta_{g1} = \frac{m_{g1}}{m_{z1}} \end{cases} \tag{8}$$

where m_{g1} is the mass of pod pepper lost by ground drop in the simulation, g; m_{z1} is the total mass of pod pepper fed in the simulation, 373.7 g; m_{s1} is the mass of pod pepper successfully harvested in the simulation, g; η_{g1} is the simulated nominal ground drop loss rate of pod pepper, %.

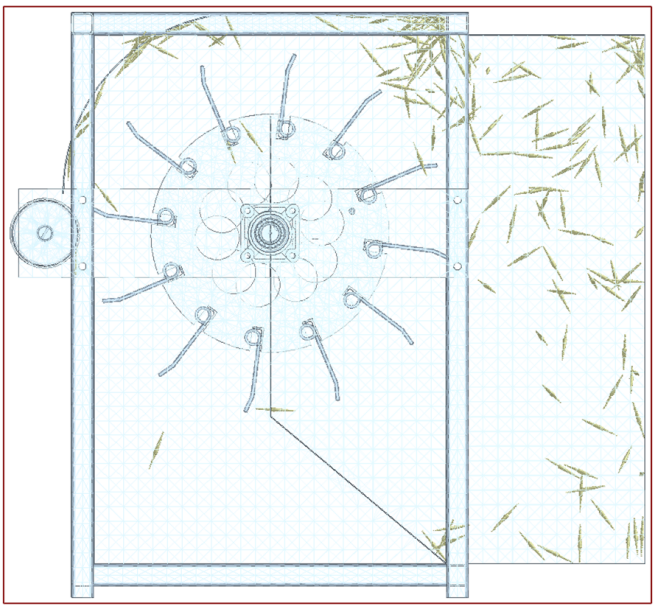

Figure 9. Schematic diagram of the simulation process of pod-pepper-picking bench.

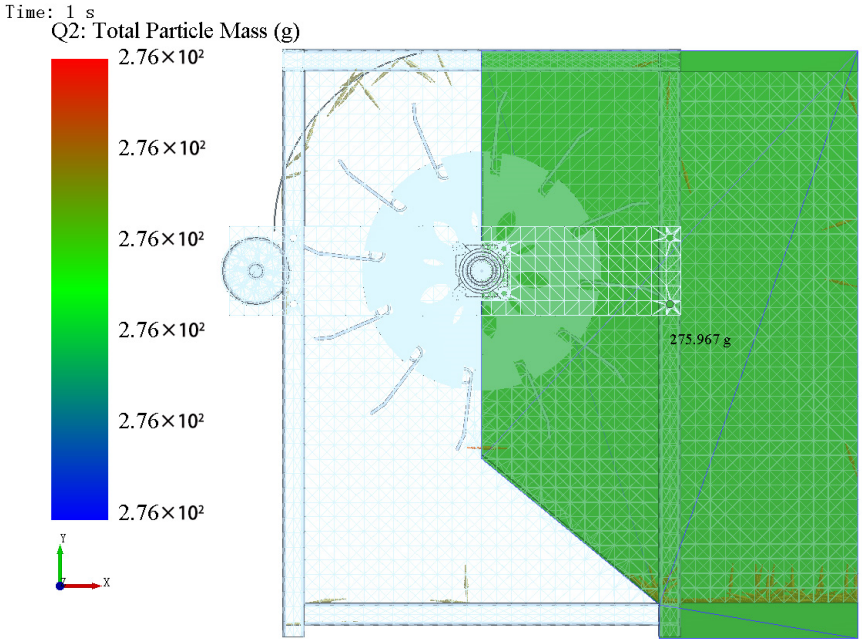

Figure 10. Weight statistics of pod peppers during simulation process.

3. Results

3.1. The Plackett–Burman Test Identifies Significant Influencing Factors

By establishing a multi-finger synergistic bionic finger arrangement scheme on the picking drum, four factors that may have a significant impact on the ground drop loss rate (η_{g1}) of pod pepper in the EDEM simulation of the pepper-picking bench and their levels were identified (Table 2), and it is proposed to further determine the three factors that have the most significant influence through the Plackett–Burman experimental design.

Table 2. Factors and levels of Plackett–Burman test.

Factor	Level		
	−1	**0**	**+1**
Picking drum speed V' (rpm)	150	200	250
pod pepper feeding speed V'' $(mm \cdot s^{-1})$	500	1000	1500
Picking finger bend angle C (°)	90	135	180
The number of rows of snap fingers in each group N	2	3	4

Design Expert 12 was used to carry out the Plackett–Burman experimental design of the EDEM simulation of the picking platform, specifically the evaluation index of the ground drop loss rate (η_{g1}) of pepper in the simulation, and screen out the three factors that have the most significant impact on the evaluation index among V', V'', C, and N. Each group of simulation experiments was repeated 3 times, and the average value of η_{g1} was obtained. The experimental design and corresponding simulation results are shown in Table 3.

Table 3. Design and results of Plackett–Burman test.

Serial Number	V'	V''	C	N	η_{g1} (%)
1	1	1	1	−1	13.33
2	−1	1	−1	1	8.33
3	1	−1	1	1	16.11
4	−1	1	1	−1	6.67
5	−1	−1	−1	1	8.89
6	−1	−1	1	−1	10.00
7	1	−1	−1	−1	20.00
8	1	1	−1	−1	10.00
9	1	1	−1	1	13.33
10	−1	1	1	1	5.56
11	1	−1	1	1	15.56
12	−1	−1	−1	−1	12.78
13	0	0	0	0	9.44

The parameter significance analysis was carried out on the test results. From the analysis results (Table 4), it can be seen that the most significant parameters affecting the ground drop loss rate η_{g1} of pod pepper in the simulation are picking drum speed V', pod pepper feeding speed V'', and picking finger bending angle C.

Table 4. Significance analysis of Plackett–Burman test parameters.

Factor	Effect	Mean Square Sum	Influence Rate (%)	Significance Ranking
V'	6.02	108.60	48.32	1
V''	−4.35	56.85	25.30	2
C	−1.02	3.10	1.38	3
N	−0.83	2.08	0.93	4

3.2. The Steepest Climbing Test to Determine the Optimization Interval of Significant Parameters

Through the significance analysis of the parameters of the Plackett–Burman test, it was determined that the order of the most significant parameters is V', V'', and C. The influence rate of N on η_{g1} in each group was only 1.08%, and it was considered that its effect on η_{g1} was the least significant. Compared with other significant parameters, N had no significant effect on the ground drop loss rate of pepper. Therefore, in order to reduce the design difficulty and the processing cost of the later picking drum, the number of circumferential finger rows N per group is determined to be 2 rows, which is suitable for the subsequent picking bench simulation test. On this basis, η_{g1} was used as the evaluation index, and

the steepest climbing test was carried out on the three selected significant parameters, so as to determine the optimal value range of these parameters. In the simulation test, the main significance parameters V', V'', and C have value ranges of 150~250 (rpm), 500~1500 (mm·s^{-1}), and 90~180 (°), respectively, which can be divided into 6 groups of gradient values according to the series of equal differences, and the results of each group of experiments repeated 5 times were averaged. Except for N as row 2, all other irrelevant parameters remained the same as in the Plackett–Burman experiment. The design and results of the steepest climbing test are shown in Table 5. The results show that with the increase in the picking drum speed V', the pepper feeding speed V'', and the picking finger bending angle C, the ground drop loss rate η_{g1} of peppercorns in the simulation is that of first decreasing and then rising, and η_{g1} was the smallest in the fifth group of experiments (V' was 230 (rpm), V'' was 1300 (mm·s^{-1}), and C was 162 (°)), indicating that this group of experiments was close to the optimal response interval of each significant parameter. Therefore, this test group was taken as the central test point of the next response surface test; V', V'', and C in groups 4, 5, and 6 can be used as the −1, 0, and 1 levels.

Table 5. Design and results of steepest ascent test.

Serial Number	V' (rpm)	V''(mm·s^{-1})	C (°)	η_{g1} (%)
1	150	500	90	12.78
2	170	700	108	12.22
3	190	900	126	11.11
4	210	1100	144	10.56
5	230	1300	162	10.00
6	250	1500	180	10.56

3.3. Box–Behnken Response Surface Test and Analysis

Through the Plackett–Burman test and the steepest climb test, the values of V', V'', and C at the level of −1, 0, and 1 in the Box–Behnken test were determined, while the settings of other irrelevant parameters in the Box–Behnken test were consistent with those in the steepest climb test. The Box–Behnken experimental design was carried out using Design Expert 12 software, the simulation test was carried out based on the EDEM simulation model of the picking bench, and the experimental design and simulation results are shown in Table 6.

Table 6. Design and results of Box–Behnken test.

Serial Number	V'	V''	C	η_{g1} (%)
1	−1	−1	0	8.29
2	1	−1	0	13.08
3	−1	1	0	9.67
4	1	1	0	11.11
5	−1	0	−1	8.89
6	1	0	−1	13.24
7	−1	0	1	7.83
8	1	0	1	13.46
9	0	−1	−1	8.03
10	0	1	−1	10.41
11	0	−1	1	8.22
12	0	1	1	10.23
13	0	0	0	10.56
14	0	0	0	8.78
15	0	0	0	9.87
16	0	0	0	9.42
17	0	0	0	8.85

Variance analysis and multiple regression analysis was carried out on the test results and established the unary linear regression model equation (Equation (9)) of the ground drop loss rate η_{g1} and V', V'', and C of pod pepper in the simulation. The results of variance analysis of the Box–Behnken test regression model are shown in Table 7. The p-value of the model is <0.001, and the p-value of the lack-of-fit item is 0.1365 $>$ 0.05, indicating that the model is extremely significant and fits well, and no lack of fit occurs. The p-value of $V' < 0.01$, indicating that it has a significant influence on the ground drop loss rate η_{g1} of pod pepper in the simulation. The p-values of V'' and C are all $>$ 0.05, indicating that the feeding speed of pod pepper and the bending angle C of picking fingers have no significant effect on η_{g1}. In summary, the regression model fits well, and has high reliability and credibility.

$$\eta_{g1} = -15.4592 + 0.1013V' + 0.0024V'' - 0.0058C \quad (9)$$

Table 7. Design and results of Box–Behnken test.

Source of Variance	Mean Square Sum	Degrees of Freedom	Mean Square	F-Value	*p*-Value
Model	34.74	3	11.58	8.28	0.0024 ***
V'	32.85	1	32.85	23.50	0.0003 ***
V''	1.80	1	1.80	1.29	0.2763
C	0.0861	1	0.0861	0.0616	0.8079
residual	18.17	13	1.40		
Lack of fit	15.97	9	1.77	3.21	0.1365
pure error	2.21	4	0.5519		
sum	52.91	16			

Note: *** indicates significant ($0.01 < p < 0.05$); indicates very significant ($p < 0.01$).

Since the finger bending angle C has no significant effect on η_{g1}, in order to facilitate processing and reduce manufacturing costs, it is proposed to pick the finger bending angle C according to the general picking finger structure, and the finger bending angle C is 162°. The optimization module in Design Expert software was used, the ground drop loss rate η_{g1} of pod pepper in the simulation was taken as the minimum value, and the optimization solution with constrained target was carried out (Equation (10)). The optimal parameter value combination of V', V'', and C was obtained by solving with a picking drum speed of 210 rpm, a pod pepper feeding speed of 1100 mm·s^{-1}, and a picking finger bending angle of 162° (consistent with the optimization results shown in Figure 11). The optimized layout parameters obtained through simulation were applied to the tooth arrangement of the picking drum, and the picking effect was greatly improved. At this time, the pepper loss rate is 7.50% in the corresponding simulation.

$$\begin{cases} Minimize\{\eta_{g1}(V', V'', C)\} \\ \begin{cases} 210 \le V' \le 250 \\ 1100 \le V'' \le 1500 \\ C = 162 \end{cases} \end{cases} \quad (10)$$

3.4. Field Verification Test

The three parameters obtained after simulation optimization were applied to the design of the actual picking device and installed on the pod-pepper-picking machine for field experiments to verify the reliability of the parameters obtained after simulation optimization by comparing the picking effect data of simulation and experiment. In order to verify the above optimal parameter combination, pod pepper farmland in Shouxian Town, Fengxian County, Xuzhou City, Jiangsu Province, China was selected as the experimental site, and a crawler self-propelled pod pepper harvester equipped with the pepper-picking

device was selected for the field experiment of harvesting pod pepper (Figure 11). The variety of pod pepper used in the test is Tianyu pod pepper (average plant height 653 mm, plant width 228 mm, plant spacing 258 mm, row spacing 720 mm, planting density about 71,765 plants/hm^2, average fruiting height 364~613 mm, average fruiting number 96 per plant, pod pepper moisture content 52.5%). During the test, according to the optimal parameter combination, the corresponding pod-pepper-picking drum speed was set to 2105 rpm, the forward speed of the pod pepper harvester was 1.1 to 0.1 m·s^{-1}, and the bending angle of the picking fingers was 162°. We assembled the picking drum with the arrangement scheme of picking fingers whose row number N was 2 (see Figure 12). In the experiment, two rows of pod peppers with the best growing conditions were selected for harvesting test. The harvester normally drove a distance of 20 m, and the nominal ground drop loss rate of pod peppers in this interval was counted, and the experiment was repeated three times.

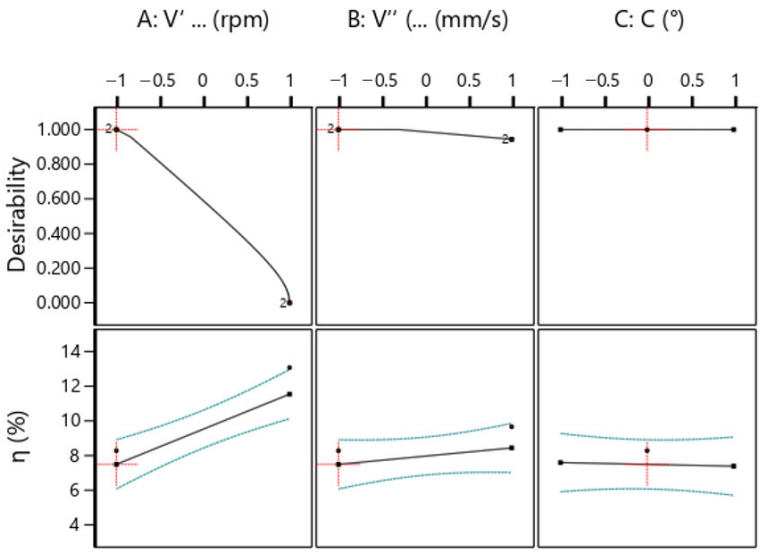

Figure 11. Analysis of optimization results of Box–Behnken experiment.

Figure 12. Field test and pod-pepper-picking device.

Comparing Equation (8), it can be seen that the ground drop loss rate η_{g1} of pod pepper in the simulation should be consistent with the nominal ground drop loss rate η_{d1} of pod pepper, then η_{d1} can be further calculated by Equation (11) to obtain 7.85%, that is,

the relative error between the ground drop loss rate η_{g1} of pod pepper in the simulation and the nominal ground drop loss rate η_{d1} of pod pepper is 4.46%. Therefore, after the field verification test, it can be considered that the optimal parameter combination value of the pepper-picking device has good reliability, and the picking device can obtain the smallest ground drop loss rate of pod pepper under the conditions that the picking drum speed V' is 210 rpm, the feeding speed of pod pepper V'' is 1100 mm·s^{-1}, the picking finger bending angle is 162°, and the number of circumferential finger rows N per group is 2.

$$\eta_{g1} = \frac{m_d}{m_z - m_g} \times 100\% \tag{11}$$

where η_{d1} is the nominal ground drop loss rate of pod pepper, %; m_d is the mass of pepper fruit that fell on the ground after harvest, g; m_z is the total mass of pepper, g; m_g is the mass of pepper remaining (unpicked) on the branch after harvest, g.

4. Discussion

In order to improve the clean rate of pepper and reduce the loss rate, the bionic finger and bionic finger arrangement method were designed based on human fingers and flexibly applied to the self-designed drum pepper-picking device. The discrete element simulation experiment was carried out with an orthogonal experiment of the response surface to simulate pepper picking to optimize the design parameters of the picking device, and the optimal parameter values of V', V'', and C were solved; the speed of the picking drum V' was 210 rpm, the feeding speed of pod pepper V'' was 1100 mm·s^{-1}, and the bending angle of the picking finger was 162°. At this time, the corresponding simulation in the simulation of pod pepper ground drop loss rate η_{g1} is 7.50%. Finally, the working effect of the optimized picking device was verified by field test; the nominal ground drop loss rate of pepper in the field test η_{d1} was 7.85%, and the relative error between the drop loss rate of the simulation and experiment test was 4.46%.

In order to reduce the loss rate of pepper and improve the sub-profit rate during the separation of pepper stems in the pepper harvester, Shin et al. replaced the traditional elastic teeth with a brush, and the loss rate of the four-axis drum was increased by 3.7% compared with the three-axis drum during the test, indicating that improving the flexibility of the parts in contact with the pepper and reducing the number of contacts between the pepper and the rigid object could reduce the loss rate of the pepper [21]. Gupt et al. found that appropriately reducing the rotation speed of the picking drum can reduce the loss rate of peppers when using a comb-tooth picking device to pick peppers [22]. However, in order to ensure a high picking efficiency, an appropriate value needs to be selected. In this paper, the appropriate rotational speed of the picking device is determined by orthogonal experiments, which has reference significance for the selection of appropriate rotational speeds for other forms of picking rolling. Kim et al. designed a small double-helix pepper picker and measured the pepper drop loss rate [23]. The double-helix picking form was designed to avoid frontal collisions between peppers and rigid objects to reduce the loss rate, but its surface is still rigid material. Du et al. calibrated the DEM parameters of pepper, which effectively laid the foundation for the simulation accuracy of this paper [19,24,25]. The profiling teeth in this paper can not only avoid the frontal collision between the rigid body and the pepper to reduce the breakage rate of the pepper, but they also have a higher harvesting efficiency than the double helix and other picking forms, and the parameters are optimized by the DEM simulation method, which effectively improves the picking efficiency of the pepper and reduces the ground drop loss rate [26].

The vigorous development of bionics provides a new idea for the research on the picking device of pod pepper harvester and its loss reduction technology. Starting from the research on the material characteristics and mechanical parameters of pod pepper, human fingers were used as a bionic prototype to analyze and refine the motion configuration and material assembly of fingers when picking pod pepper. The arrangement scheme and material assembly of the fingers on the picking drum were optimized, so as to establish

the bionic loss model of the picking drum. Based on this model, the optimization of the technical parameters of the picking device was carried out, and the field test of pod pepper harvesting was carried out, so as to develop the pod pepper harvester picking device with low ground drop loss rate and low breakage rate, which provides a new idea for the development of low-loss pod pepper harvester.

5. Conclusions

A biomimetic design of the harvesting device for pod pepper was presented in this article, and the design parameters of the harvesting device were optimized through Box–Behnken experiments. Through the design and analysis of Box–Behnken experiment based on the EDEM simulation experiment of the pepper-picking bench, the factors of the ground drop loss of pod pepper and their optimal parameter combination values were obtained; the picking drum speed is 210 rpm, the pod pepper feeding speed is 1100 mm·s^{-1}, the bending angle C of picking fingers is 162°, and the number of rows N of fingers in each group is 2. The drop loss rate of pepper in the simulation and test is 7.50% and 7.85%, respectively, and the relative error between the simulation and verification test was 4.46%. The error between the simulation and experiment is within an acceptable range, and the results of simulation optimization are reliable. The experimental results prove that the harvesting device designed in this paper has low ground drop loss rate of pepper.

Author Contributions: Conceptualization, C.D. and X.W.; methodology, C.D.; software, C.D.; validation, C.D., W.F. and D.H.; formal analysis, W.F.; investigation, X.W.; resources, X.W.; data curation, C.D.; writing—original draft preparation, C.D. and W.F.; writing—review and editing, X.W., D.H., X.W. and X.C.; visualization, C.D.; supervision, X.C.; project administration, X.W.; funding acquisition, X.W. All authors have read and agreed to the published version of the manuscript.

Funding: This study was supported by Jiangsu Province Modern Agricultural Machinery Equipment and Technology Demonstration and Promotion Project (No. NJ2020-14), Jiangsu Province and Education Ministry Co-sponsored Synergistic Innovation Center of Modern Agricultural Equipment (No. XTCX2003), Project of the Agricultural Equipment Faculty of Jiangsu University (No. NZXB20200104), the National Key Research and Development Project (No.2022YFD2002403), A Project Funded by the Priority Academic Program Development of Jiangsu Higher Education Institutions (PAPD).

Data Availability Statement: The data presented in this study are available in this article. All authors confirm that the data in this manuscript are available and original.

Conflicts of Interest: The authors declare no conflicts of interest.

References

1. Funk, P.A.; Walker, S.J. Evaluation of five green chile cultivars utilizing five different harvest mechanisms. *Appl. Eng. Agric.* **2010**, *26*, 955–964. [CrossRef]
2. Chen, Y.; Hu, J.; Yuan, Y. *Research of the Comb-Type Picking Device for Chili Pepper*; Chinese Society for Agricultural Machinery: Hangzhou, China, 2012; pp. 942–948.
3. Ning, Z.; Luo, L.; Ding, X.; Dong, Z.; Yang, B.; Cai, J.; Chen, W.; Lu, Q. Recognition of sweet peppers and planning the robotic picking sequence in high-density orchards. *Comput. Electron. Agric.* **2022**, *196*, 106878. [CrossRef]
4. Liu, S.; Liu, M.; Chai, Y.; Li, S.; Miao, H. Recognition and Location of Pepper Picking Based on Improved Yolov5s and Depth Camera. *Appl. Eng. Agric.* **2023**, *39*, 179–185. [CrossRef]
5. Deng, L.; Liu, T.; Jiang, P.; Qi, A.; He, Y.; Li, Y.; Yang, M.; Deng, X. Design and Testing of Bionic-Feature-Based 3D-Printed Flexible End-Effectors for Picking Horn Peppers. *Agronomy* **2023**, *13*, 2231. [CrossRef]
6. Xie, F.; Luo, X.; Su, A.; Wu, M. Contrastive Experiment on Threshing by Using Rigid Wire-Loop, Rigid Pole Tooth and Flexible Pole Tooth. *J. Hunan Agric. Univ. (Nat. Sci.)* **2005**, *31*, 648–651. [CrossRef]
7. Zou, D.; Maimaiti Turson, A.; Han, C.; Li, Q.; Li, Y.; Zhang, J. Design and experiment of picking platform of pepper harvester. *J. Agric. Mech. Res.* **2022**, *44*, 105–109. [CrossRef]
8. Li, X.; Li, Y.; Gao, H.; Qiu, Z.; Ma, F.; Gao, L. Bionic Threshing Process Analysis of Seed Corn Kernel. *Trans. Chin. Soc. Agric. Mach.* **2011**, *42*, 99–103. [CrossRef]
9. Sun, G. Study on Optimization of Snapping Roller Based on Bionic Corn Ear Picking Device. Master's Thesis, Jilin University, Changchun, China, 2018.
10. Wu, T. Bionic Design and Simulation Analysis of Corn Stubble Collector. Master's Thesis, Jilin University, Changchun, China, 2015.

11. Zhang, L.; Lin, C.; Hou, G.; Yan, M.; Yu, J.; Zhang, Q. Design and experiment of bionic threshing unit for corn with high moisture content. *J. Agric. Mech. Res.* **2021**, *43*, 126–131. [CrossRef]
12. Wei, W.; Dai, F.; Zhang, F.; Zhao, W.; Zhang, S.; Shi, R. Design of bionic harvest cutting table of flax in dry area. *J. Chin. Agric. Mech.* **2018**, *39*, 44–48, 57. [CrossRef]
13. Li, X.; Wu, K.; Jin, X.; Gao, C.; Gao, L. Analysis on discrete process of kernels caused by beak pecking corn ear by simulating threshing. *Trans. Chin. Soc. Agric. Eng. (Trans. CSAE)* **2015**, *31*, 34–40. [CrossRef]
14. Islam, M.N.; Iqbal, M.Z.; Ali, M.; Chowdhury, M.; Kabir, M.S.N.; Park, T.; Kim, Y.-J.; Chung, S.-O. Kinematic Analysis of a Clamp-Type Picking Device for an Automatic Pepper Transplanter. *Agriculture* **2020**, *10*, 627. [CrossRef]
15. Lu, J.; Xiang, J.; Liu, T.; Gao, Z.; Liao, M. Sichuan Pepper Recognition in Complex Environments: A Comparison Study of Traditional Segmentation versus Deep Learning Methods. *Agriculture* **2022**, *12*, 1631. [CrossRef]
16. Hu, S.; Hu, M.; Yan, W.; Zhang, W. Design and Experiment of an Integrated Automatic Transplanting Mechanism for Picking and Planting Pepper Hole Tray Seedlings. *Agriculture* **2022**, *12*, 557. [CrossRef]
17. Zhang, N.; Zhang, G.; Liu, H.; Liu, W.; Wei, J.; Tang, N. Design of and Experiment on Open-and-Close Seedling Pick-Up Manipulator with Four Fingers. *Agriculture* **2022**, *12*, 1776. [CrossRef]
18. Fang, W.; Wang, X.; Han, D.; Chen, X. Review of Material Parameter Calibration Method. *Agriculture* **2022**, *12*, 706. [CrossRef]
19. Du, C.; Han, D.; Song, Z.; Chen, Y.; Wang, X. Calibration of contact parameters for complex shaped fruits based on discrete element method: The case of pod pepper (*Capsicum annuum*). *Biosyst. Eng.* **2023**, *226*, 43–54. [CrossRef]
20. Liu, F.; Zhang, J.; Chen, J. Modeling of flexible wheat straw by discrete element method and its parameters calibration. *Int. J. Agric. Biol. Eng.* **2018**, *11*, 42–46. [CrossRef]
21. Shin, S.-Y.; Kim, M.-H.; Cho, Y.; Kim, D.-C. Performance Testing and Evaluation of Drum-Type Stem-Separation Device for Pepper Harvester. *Appl. Sci.* **2021**, *11*, 9225. [CrossRef]
22. Gupta, C.; Tewari, V.K.; Machavaram, R. Evaluation of a Laboratory-based Prototype of a Comb-type Picking Mechanism for Chili Pepper Harvester. *J. Biosyst. Eng.* **2022**, *47*, 69–78. [CrossRef]
23. Kim, T.-H.; Kim, D.-C.; Cho, Y. Performance Comparison and Evaluation of Two Small Chili Pepper Harvester Prototypes That Attach to Walking Cultivators. *Appl. Sci.* **2020**, *10*, 2570. [CrossRef]
24. Nam, J.S.; Byun, J.H.; Kim, T.H.; Kim, M.H.; Kim, D.-C. Measurement of mechanical and physical properties of pepper for particle behavior analysis. *J. Biosyst. Eng.* **2018**, *43*, 173–184.
25. Shi, L.; Zhao, W.; Sun, B.; Sun, W. Determination of the coefficient of rolling friction of irregularly shaped maize particles by using discrete element method. *Int. J. Agric. Biol. Eng.* **2020**, *13*, 15–25. [CrossRef]
26. Yuan, X.; Yang, S.; Jin, R.; Zhao, L.; Dao, E.; Zheng, N.; Fu, W. Design and experiment of double helix pair roller pepper harvesting device. *Trans. Chin. Soc. Agric. Eng.* **2021**, *37*, 55–61.